

DENSITY AND TEMPERATURE PROFILES OBTAINED BY LIDAR BETWEEN 35 AND 70 KM

Alain Hauchecorne and Marie-Lise Chanin

Service d'Aéronomie du CNRS, 91370, Verrières-le-Buisson, France

Abstract. A lidar system based at the Haute-Provence Observatory (44°N, 6°E) has been used to obtain night-time density and temperature profiles in the altitude range 35-70 km. If the lidar results are normalized to an in-situ rocket sounding from 35 to 40 km, the lidar and rocket profiles are in quite good agreement up to about 50 km. Differences are sometimes noted around 55 km, and these could possibly be caused by an aerosol layer.

Introduction

Light scattered from a laser beam has been observed up to 100 km for quite a number of years (Mc Cormick et al., 1967 ; Sandford, 1967 ; Kent and Wright, 1970) with the purpose of measuring atmospheric densities. An extensive study of mesospheric density was carried out between 70 and 100 km and indicated the existence of tidal modes (Kent and Keenliside, 1975).

This paper describes the density and temperature results obtained from a ground based lidar between 35 and 70 km and presents a comparison with in-situ rocket sounding measurements. The good agreement between both types of results shows promise that ground lidar technique can provide these types of data with high resolution and accuracy.

Method

The light of a laser pulse sent vertically into the atmosphere is backscattered by the air molecules and by the aerosols. The altitude range of the measurements is divided by the height range of the collection gate into n layers of thickness Δz . The measured signal backscattered in the i th altitude layer ($z_i - \Delta z/2, z_i + \Delta z/2$) is then given by the lidar equation :

$$N(z_i) = \frac{N_0 A K T^2(z_0, z_i)}{4\pi(z_i - z_0)^2} |n_r(z_i)\beta_r + n_m(z_i)\beta_m| \Delta z \quad (1)$$

where N_0 is the number of emitted photons, $n_r(z_i)$ and $n_m(z_i)$ the air molecules and aerosols concentrations, β_r and β_m the Rayleigh and Mie backscattering cross-sections, z_0 the altitude of the lidar site, A the telescope area, $T^2(z_0, z_i)$ the atmospheric transmission, K the optical efficiency of the lidar system. The scattering ratio defined as :

$$R(z_i) = \frac{n_r(z_i)\beta_r + n_m(z_i)\beta_m}{n_r(z_i)\beta_r} \quad (2)$$

is used to estimate the contribution of the Mie diffusion in the backscattered signal $N(z_i)$.

Earlier lidar measurements at $\lambda = 694.3$ nm (Mc Cormick et al., 1978 ; Russel and Hake, 1977) have shown that the scattering ratio tends towards unity at 35 km. The wavelengths used in this study ($\lambda = 590$ nm, $\lambda = 670$ nm), chosen for the detection of sodium and lithium atoms above 80 km, lead to somewhat smaller values of the scattering ratio. We will initially assume that the scattering ratio is unity from 35 to 80 km, and later discuss the possible existence of an aerosol layer in this altitude range.

The atmospheric transmission term $T^2(z_0, z_i)$, taking into account ozone absorption and molecular extinction, is assumed to be constant between 35 and 80 km with an accuracy of 0.4%. But uncertainties on the atmospheric transmission from the ground to 35 km, the laser flux and the optical efficiency of the lidar system prevent the measurement of the absolute density. Normalization of the density data have to be made either using a model, or other experimental data. The density profiles are normalized from 35 to 40 km using an absolute profile obtained either from a model (CIRA, 1972) or experimentally. The relative uncertainty on the density profile is assumed to be equal to the statistical standard error :

$$\delta\rho(z_i) / \rho(z_i) = |N(z_i) + N_m|^{1/2} / N(z_i) \quad (3)$$

where $\rho(z_i)$ and $\delta\rho(z_i)$ are respectively the atmospheric density and its standard deviation in the i th altitude layer and N_m the background noise.

The temperature profile is computed from the density profile assuming that the atmosphere obeys the perfect gas law and is in hydrostatic equilibrium. This second assumption implies that atmospheric turbulence does not affect the mean air density, which is the case considering the temporal and spatial resolutions of the lidar data. The constant mixing ratio of the major atmospheric constituents (N_2 , O_2 and Ar) and the negligible value of the H_2O mixing ratio justify the choice of a constant value M for the air mean molecular weight. The air pressure $P(z)$, density $\rho(z)$ and temperature $T(z)$ are then related by :

$$P(z) = \frac{R \rho(z) T(z)}{M} \quad (4)$$

$$dP(z) = -\rho(z) g(z) dz \quad (5)$$

where R is the universal gas constant and $g(z)$ the acceleration of gravity. The combination of Eq. 4 and Eq. 5 leads to :

$$\frac{dP(z)}{P(z)} = -\frac{M g(z)}{R T(z)} dz = d(\text{Log } P(z)) \quad (6)$$

If the acceleration of gravity and the temperature are assumed to be constant in the i th layer, the pressure at the bottom and top of the

TABLE I. Characteristics of the lidar system

Emitter :		
Measured alkali	Sodium	Lithium
Energy per pulse	1 J	0.8 J
Wavelength	590 nm	670 nm
Linewidth	8 pm	6 pm
Beam divergence	1.10 ⁻³ rad	1.10 ⁻³ rad
Divergence after collimation	1.10 ⁻⁴ rad	1.10 ⁻⁴ rad
Pulse duration	4 μs	3.5 μs
Repetition rate	0.5 Hz	1 Hz
Receiver :		
Telescope area	0.5 m ²	
Beamwidth	5.10 ⁻⁴ rad	
Linewidth	0.5 nm	

layer are related by :

$$\frac{P(z_i - \Delta z/2)}{P(z_i + \Delta z/2)} = \exp \frac{M g(z_i)}{R T(z_i)} \Delta z \quad (7)$$

and the temperature is expressed as :

$$T(z_i) = \frac{M g(z_i) \Delta z}{R \text{Log} \left| \frac{P(z_i - \Delta z/2)}{P(z_i + \Delta z/2)} \right|} \quad (8)$$

The density profile is measured up to the *n*th layer (about 80 km). The pressure at the top of this layer is fitted with the pressure of the CIRA 1972 model $P_m(z_n + \Delta z/2)$ for the corresponding month and latitude. The top and bottom pressures of the *i*th layer are then :

$$P(z_i + \Delta z/2) = \sum_{j=i+1}^n \rho(z_j) g(z_j) \Delta z + P_m(z_n + \Delta z/2) \quad (9)$$

$$P(z_i - \Delta z/2) = P(z_i + \Delta z/2) + \rho(z_i) g(z_i) \Delta z \quad (10)$$

Let *X* be :

$$X = \frac{\rho(z_i) g(z_i) \Delta z}{P(z_i + \Delta z/2)} \quad (11)$$

The temperature is then :

$$T(z_i) = \frac{M g(z_i) \Delta z}{R \text{Log} (1 + X)} \quad (12)$$

The statistical standard error on the temperature is :

$$\frac{\delta T(z_i)}{T(z_i)} = \frac{\delta \text{Log} |1 + X|}{\text{Log} |1 + X|} = \frac{\delta X}{(1 + X) \text{Log} (1 + X)} \quad (13)$$

with

$$\left(\frac{\delta X}{X}\right)^2 = \left|\frac{\delta \rho(z_i)}{\rho(z_i)}\right|^2 + \left|\frac{\delta P(z_i + \Delta z/2)}{P(z_i + \Delta z/2)}\right|^2 \quad (14)$$

$$\delta P(z_i + \Delta z/2)^2 = \sum_{j=i+1}^n |g(z_j) \delta \rho(z_j) \Delta z|^2 + |\delta P_m(z_n + \Delta z/2)|^2 \quad (15)$$

The contribution of the extrapolated pressure at 80 km $P_m(z_m + \Delta z/2)$ on the local pressure below decreases rapidly with altitude, and its influence on the temperature determination is small below 65 km. Then the term *X* represents a ratio of experimental density values from which absolute temperature can be deduced even though the density measurements are only relative.

Lidar system description

The data reported here were obtained with the lidar system set up at the Haute Provence Observatory (43°56'N, 5°43'E). This system was developed for measurements of atmospheric alkalis (sodium and lithium) (Mégie and Blamont, 1977 ; Mégie et al., 1978 ; Jégou and Chanin, 1980). The emitter part consists of two flash-pumped dye lasers ; the light is sent vertically through a collimator into the atmosphere. The receiver includes a 80 cm diameter telescope and an analogic and photoelectron counting detection system. Table I summarizes the present characteristics of the lidar system. The data are now still limited to night-time (solar elevation < - 10°). A rotating disk protects the photocatode from overloading during the first 200 μs. As a consequence the backscattered signal is only measured above 30 km.

Results

Data collected for 27 nights during the period extending from october 1978 to september 1979 have been studied. We only present in this paper the data collected during the three nights for which in-situ temperature measurements were available during the preceding or the following day. These were obtained by probes carried by ARCAS type rockets launched from the Centre d'Essai des Landes (44°20'N, 1°15'W). The data were recorded during the descent of the probe under a parachute. The temperature is measured with a tungsten wire and the density and pressure are inferred from this measurements (Villain and Loitière, 1974). The temperature error is given as 1°C at 55 km and 2°C at 65 km. The rocket soundings are made during daytime and the lidar sites are 560 km distant but situated at the same latitude. The wind is nearly zonal during all these experiments, and thus the

TABLE 2. Presentation of lidar and rocket data

Date	Dec.18-19 1978	July 9-10 1979	July 15-16 1979
Lidar :			
Beginning	20H, GMT	22H	21H
End	4H	3H	3H
Wavelength	670 nm	590 nm	590 nm
Number of pulses	13800	6900	4500
Rocket sounding :			
Time	15H	11H	16H
Zonal wind (East-ward positive, 35, 60 km) ms ⁻¹	+70,+140	25,-60	-20,-35

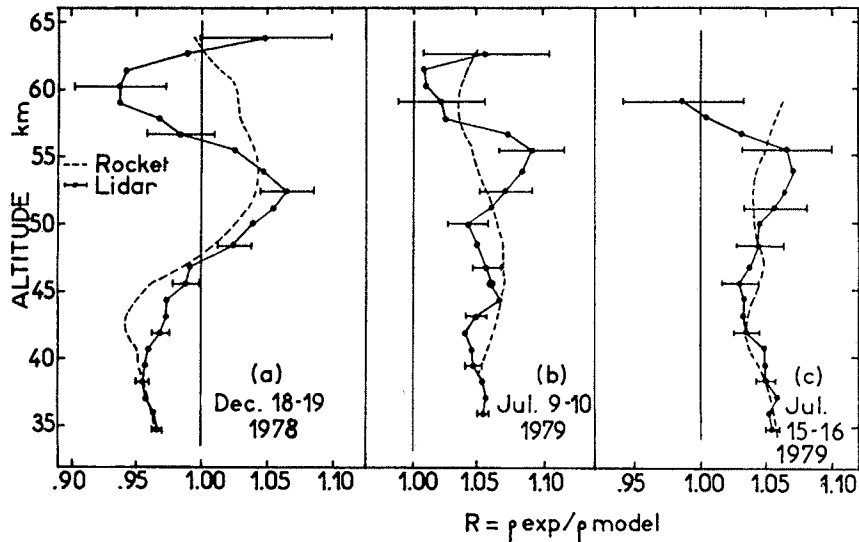


Fig. 1. Ratio of the experimental densities obtained by lidar and rocket to the CIRA 1972 model corresponding to the 1st of December (a) and the 1st of July (b and c) and interpolated to 44°N. Lidar profiles are normalized to rocket profiles between 35 and 39 km. Horizontal bars indicate the standard deviation of lidar results.

same air mass will be over both sites within a few hours. The characteristics of the data to be compared are summarized in Table 2.

The height resolution of the lidar and rocket measurements are respectively 1.2 km and 0.5 km, and have been reduced to 4.8 km by a running average in order to decrease the standard deviation.

The lidar and rocket sounding densities, ρ_L and ρ_R , are compared with the density of the CIRA 1972 model ρ_M selected for the month of the measurements and interpolated to 44°N. The ratios of the density measured by both methods to the model :

$$R_L = \rho_L / \rho_M, \quad R_R = \rho_R / \rho_M \quad (16)$$

are presented on Figure 1 for the three comparisons. Lidar density has been normalized to rocket results in the lower part of the profile (35-39 km). On this figure, the vertical pro-

files of density and temperature are limited to below the height for which the relative standard deviation of the lidar results reaches 5%, but the density results up to 80 km are used for the temperature determination.

The experimental density profiles obtained by both techniques are in quite good agreement below 50 km in all cases, even when the density is disturbed as in case a. An oscillation around the model is observed by the two independent techniques : vertical wavelength of 20 to 10 km can be measured in case a and b.

The lidar and rocket measured temperature are now compared with the appropriate CIRA 1972 model. In the case c the experimental difference stays within the standard deviation of the lidar data, and in general the agreement is satisfactory up to 50 km. For the three examples the night-time lidar temperature is 8 to 10°C lower than the day-time rocket data at 52 - 55 km. This difference, associated with the maxima

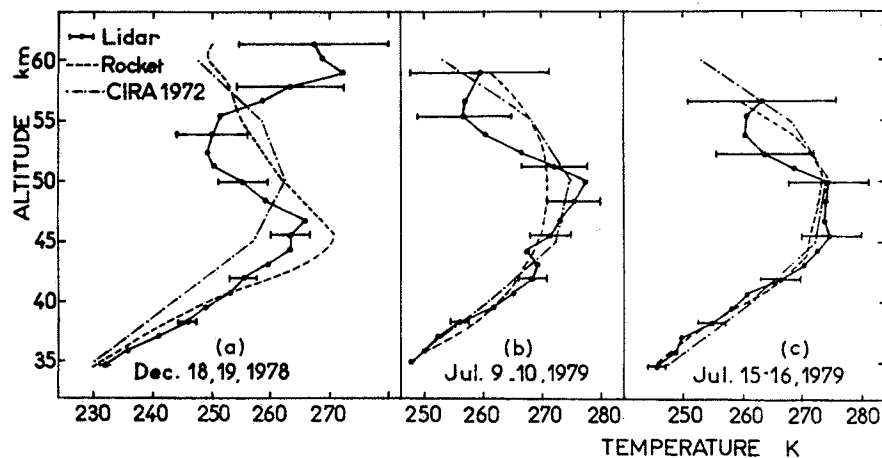


Fig. 2. Experimental temperature from lidar and rocket data compared with the corresponding CIRA 1972 model. Horizontal bars indicate the standard deviation of lidar results.

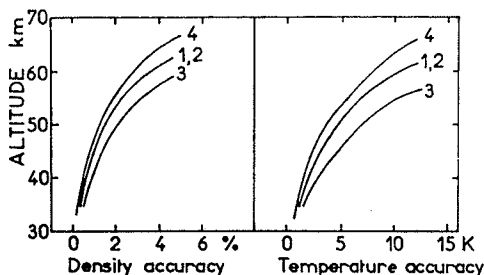


Fig. 3. Density and temperature accuracy of lidar profiles. Numbers refer to the night of the measurement: 1; December 18-19, 1978; 2; July 9-10, 1979; 3; July 15-16, 1979; 4; September 1-2, 1979.

observed on the density around these altitudes, could also be attributed to an aerosol layer at that level, which could increase the scattering ratio. Indications of such a layer have been obtained earlier. (Rössler, 1968; Cunnold et al., 1973). If one assumes that the scattering ratio is 1.05 (or 1.10) at 52-55 km and this is ignored in the density analysis, the computed temperature would be too low by 10°C (20°C) in the aerosol layer and too high by 5°C (10°C) at 50 km and 2°C (4°C) at 40 km.

Since obtaining the data presented in Figures 1 and 2, improvements involving the reduction of the divergence and the field of view have been incorporated at the lidar station to increase the accuracy. As an example, we present on Figure 3 the standard error of the density and temperature measurements, for a vertical resolution of 5 km, for the 3 nights of data reported in this paper and for the data obtained on September 1, 1979 with 14 600 laser pulses at 670 nm. During that period of measurements the magnitude of the error bar has been reduced by about 25%. Such improvement in the accuracy has increased the range of the measurements by about 4 km: as an example, for a maximum standard error of 5% in density measurement, the altitude range is now up to 66 km.

Conclusion

Lidar vertical soundings of the atmosphere are shown to allow the determination of density and temperature of the upper stratosphere and lower mesosphere. The comparison with rocket sounding profiles are quite satisfactory up to 50 km provided that each lidar density profile is normalized to match the corresponding rocket profile from 35 to 40 km. Above that level the possible presence of an aerosol layer should be cleared by using a two wavelengths lidar. In two cases, oscillations with vertical wavelengths of 10 to 20 km can be observed if the density is compared to the model. These oscillations are also present in the first rocket profile. In order to obtain absolute measurements of density, a good reference is needed for normalization in the lower part of the profile, as the density at 35 km may differ by more than 5% from the model. If such a normalization is made, and if the aerosol perturbation is either negligible or removed, the present characteristics of the lidar system allow the determination of the mean density during one night with an accuracy varying

from 0.3% at 35 km to 5% at 66 km. The accuracy of the inferred temperature, independent of the density normalization, varies from 0.8°C at 35 km to 12°C at 66 km. Again, these temperature errors do not include any possible aerosol effect.

Acknowledgments. We wish to thank C. Fehrenbach, the Director of the Haute Provence Observatory, for his hospitality. We are grateful to all the members of the lidar team of the Service d'Aéronomie (CNRS) and particularly to J.P. Jegou, J.P. Schneider and F. Syda who collected the data used in this study. The rocket sounding data have been gracefully provided by the Météorologie Nationale (EERM).

This work was supported by the DRET under contracts N° 77-280 and 79-442.

References

- CIRA 1972, Cospar International Reference Atmosphere 1972, COSPAR Committee for CIRA, Akademie Verlag, Berlin, 450 pp. 1972.
- Cunnold, D.M., C.R. Gray, and D.C. Merritt, Stratospheric aerosol layer detection, J. Geophys. Res., **78**, 920-931, 1973.
- Jegou, J.P., and M.L. Chanin, Lidar measurements of atmospheric lithium, to be submitted to Planet. Space Sci., 1980.
- Kent, G.S., and W. Keenliside, Laser radar observations of the $\theta_3^{\omega, \delta}$ Diurnal atmospheric tidal mode above Kingston, Jamaica. J. Atmos. Sci., **32**, 1663-1666, 1975.
- Kent, G.S., and R.W. Wright, A review of laser radar measurements of atmospheric properties, J. Atmos. Terr. Phys., **32**, 917-943, 1970.
- Mc Cormick, P.D., E.C. Silverberg, S.K. Poultney, U. Van Wigh, C.O. Alley, and R.T. Bettinger, Optical radar detection of backscattering from the upper atmosphere, Nature, **215**, 1262-1263, 1967.
- Mc Cormick, M.P., T.J. Swisler, W.P. Chu, and W.H. Fuller, Jr., Post-Volcanic aerosol decay as measured by Lidar, J. Atmos. Sci., **35**, 1296-1303, 1978.
- Mégie, G., and J.E. Blamont, Laser sounding of atmospheric sodium; interpretation in terms of global atmospheric parameters, Planet. Space Sci., **25**, 1093-1109, 1977.
- Mégie, G., F. BOS, J.E. Blamont, and M.L. Chanin, Simultaneous night-time measurements of atmospheric sodium and potassium, Planet. Space Sci., **26**, 27-35, 1978.
- Rössler, F., The aerosol layer in the stratosphere, Space Research VIII, North Holland Publ. Co., 633-636, 1968.
- Russell, P.B., and R.D. Hake, Jr., The post-fuego stratospheric aerosol: lidar measurements with radiative and thermal implications, J. Atmos. Sci., **34**, 163-177, 1977.
- Sandford, M.C.W., Laser scatter measurements in the mesosphere and above, J. Atmosph. Terr. Phys., **29**, 1657-1662, 1967.
- Villain, J., and B. Loitière, Mesure du vent et de la température de la haute atmosphère, La Météorologie, **31-32**, 1-25, 1974.

(Received December 12, 1979;
accepted March 24, 1980.)